

# Ecological and genetic models of host–pathogen coevolution

STEVEN A. FRANK

*Department of Ecology and Evolutionary Biology, University of California, Irvine, CA 92717, USA*

A model is presented to analyse the forces that maintain genetic polymorphism in interactions between host plants and their pathogens. Genetic variability in hosts occurs for specific resistance to different pathogen races and variability in pathogens occurs for specific virulence to different host races. The model tracks both fluctuating population sizes and changing gene frequencies. Analyses over a range of parameters show that ecological and demographic factors, such as birth and death rates, often have a more profound effect on the amount of polymorphism than genetic parameters, such as the pleiotropic costs of resistance and virulence associated with different alleles. A series of simple measures are proposed to predict the amount of genetic polymorphism expected in particular host–pathogen interactions. These measures can be used to develop and test a comparative theory of genetic polymorphism in host–pathogen coevolution.

**Keywords:** disease, genetics, model, plants, polymorphism.

## Introduction

Genetic polymorphisms that affect disease resistance and pathogen specificity are widespread in plants (Day, 1974; Burdon, 1987). The question addressed here is why? As a first step, the forces that determine polymorphism in a simple model of host–pathogen coevolution are summarized. Emphasis is placed on measures of host and pathogen life history that can be used to test comparative hypotheses on a range of pathosystems.

The results presented here show that ecological factors, such as birth and death rates and total population sizes, have a strong influence on genetic polymorphism. The analysis therefore begins with ecological questions and progress toward questions about genetic diversity.

Six specific questions are analysed.

- 1 What determines the abundance of the host population relative to its carrying capacity?
- 2 What determines the abundance of the pathogen population and the frequency of disease?
- 3 What determines the percentage of pathogen attacks in which the host is resistant?
- 4 What determines the total fitness load of infection imposed on the host population?
- 5 What determines the amount of genetic poly-

morphism for resistance in hosts and for virulence in pathogens?

- 6 What determines the distribution of the cost of resistance in the hosts and of the cost of virulence in the pathogens?

## The model

A single haploid locus with alleles  $i = 1, \dots, n$  determines host susceptibility or resistance to particular pathogens. A single haploid locus with alleles  $k = 1, \dots, n$  determines pathogen virulence or avirulence to specific hosts. Both host and pathogen reproduce asexually. The virulence–resistance interactions are a gene-for-gene system loosely analogous with plant pathosystems (Flor, 1956; Day, 1974; Burdon, 1987), with host  $i$  resistant to pathogen  $k = i$  and susceptible to the other  $n - 1$  pathogens. The total coevolutionary system is composed of  $2n$  interacting races within a single spatial patch. At any point in time the number of host and pathogen races present may be considerably less than  $2n$ .

The model tracks the total population sizes of all host and pathogen races rather than just the relative frequencies of the host and pathogen genotypes. Thus epidemic fluctuations in population sizes and disease frequencies can be studied along with gene frequency

dynamics. The model assumes discrete Lotka–Volterra dynamics, modified from May’s (1975) equation (3.20), given by:

$$\begin{aligned}\Delta h_i &= h_i \left[ r_i(1 - h_i) - c \sum_{\substack{j=1 \\ j \neq i}}^n r_j h_j - m \sum_{\substack{k=1 \\ k \neq i}}^n p_k \right] \\ \Delta p_k &= p_k \left[ -s + b_k \sum_{\substack{i=1 \\ i \neq k}}^n h_i \right].\end{aligned}\quad (1)$$

The difference equation,  $\Delta h_i$ , is interpreted as follows. The  $h_i$  individuals in the current population can potentially increase their numbers by  $r_i h_i$  after reproduction. The  $r_i$  can be considered as two components,  $r_i = r - a_i$ , where  $r$  is the maximum rate of increase for the species and  $a_i$  is the cost of resistance associated with allele  $i$ . These offspring compete for limited resources among themselves and the offspring of the other host races, the other races having the potential to increase by the term

$$T = \sum_{\substack{j=1 \\ j \neq i}}^n r_j h_j.$$

The intraspecific competition reduces the increase in  $h_i$  by  $h_i(r_i h_i + cT)$ , where the cross-product terms  $h_i^2$  and  $h_i h_j$  are proportional to the frequency of competitive interactions. The carrying capacity for a monomorphic population is standardized to one, the competition coefficient,  $c$ , is less than or equal to one, and all other parameters are scaled accordingly. Finally, the increase in  $h_i$  is further reduced through pathogen infection by the amount  $m$  multiplied by the abundance of virulent pathogens specific for that host type.

The difference equation  $\Delta p_k$  is interpreted in a similar manner. A proportion of pathogen individuals,  $s$ , dies at the end of each time period. The number of pathogens that successfully attack a host is proportional to  $p_k$  multiplied by the abundance of susceptible hosts. Each successful pathogen produces  $b_k$  progeny that survive through the next time period. The  $b_k$  can be considered as two components,  $b_k = b - v_k$ , where  $b$  is the maximum rate of increase for the species, and  $v_k$  is the cost of virulence associated with the interactions that determine the host range of allele  $k$ .

## Mathematical analysis

A brief mathematical analysis of the dynamical system in eqn (1) is presented in this section. These equations provided a source of hypotheses that were tested by computer simulation. The meaning of these equations

and the particular hypotheses are discussed in the following section.

The full  $2n$ -dimensional system has a unique equilibrium point. This is somewhat misleading because many of the equilibrium abundances may be less than zero, so the system actually has fewer than  $2n$  dimensions and has a different equilibrium. Even if all equilibrium abundances are greater than zero, a natural system will usually maintain fewer than  $2n$  races because of stochastic extinctions and trajectories of nonequilibrium dynamics leading to extinctions. Nevertheless, analysis of the full system provides hypotheses about the factors that determine host and pathogen abundances and stability.

The equilibrium abundances for the hosts are

$$h_i^* = \overline{s/b\gamma} - s/b_i, \quad (2)$$

where the overbar denotes the average over the  $n$  races, and  $\gamma = (n-1)/n$  is the pathogen host range — the frequency of host races that a pathogen can attack. The value of  $\overline{s/b\gamma}$  is therefore the average birth rate of the pathogen population. The equilibrium total host abundance is  $n\overline{h^*} = \overline{s/b\gamma}$ .

The equilibrium abundances for the pathogens are

$$\begin{aligned}p_k^* &= \frac{(\overline{r} - r h^*)/\gamma - r_k[1 - (1-c)h_k^*]}{m} \\ &= \frac{\left[ \overline{r} - \frac{\overline{rs/b}}{n-1} + \text{Cov}(r, s/b) \right] \left| \gamma - r_k[1 - (1-c)(\overline{s/b\gamma} - s/b_k)] \right|}{m}\end{aligned}\quad (3)$$

where the covariance is taken over  $(r_i, b_i)$  pairs for the  $n$  races of hosts and pathogens. The numerator in the first form of eqn (3) is the average growth of the  $n-1$  hosts that a particular pathogen can attack, and the denominator is the severity of an infection.

The stability of the full system is difficult to analyse algebraically because of its high dimensionality. If the system is symmetric,  $r_i = r$  and  $b_k = b$  for all  $n$  races, then  $h_i^* = h^*$ ,  $p_k^* = p^*$ , and the eigenvalues can be obtained from the characteristic equation

$$\begin{aligned}\{(\lambda^2 + r h^*[1 + (n-1)c]\lambda + b m h^* p^*(n-1)^2) \\ (\lambda^2 + r h^*(1-c)\lambda + b m h^* p^*)^{n-1}\} = 0,\end{aligned}\quad (4)$$

where this equation was obtained by induction on  $n=2,3,4$  using *Mathematica* (Wolfram, 1988). When  $c=1$ , the approximate condition for instability in this discrete-time model (modulus greater than one) is  $\delta b - s > 0$ , where  $\delta$  is an undetermined constant that depends mainly on  $\gamma$ , the average host range of the pathogens. For the symmetric model,  $\delta = \gamma = (n-1)/n$ .

Because an unstable host–pathogen system is characterized by epidemics,  $\delta b - s$  is referred to here as the epidemic index.

## Computer analysis

### Methods

*Parameters of the simulations.* The parameter sets  $\{r_i\}$  and  $\{b_i\}$  were chosen so that  $\{r_i, b_i\}$  is a set of discrete points from a bivariate normal distribution with mean  $(\bar{r}, \bar{b})$ , coefficients of variation in each dimension  $CV_r$  and  $CV_b$ , and correlation  $\rho$ . If the correlation is positive, then pathogens that invest less in detoxifying host defences (high  $b$ ) tend to be resisted by relatively inexpensive host defences (high  $r$ ), whereas expensive detoxifying systems (low  $b$ ) tend to require expensive defence systems for resistance (low  $r$ ). The importance of the correlations between  $b$  and  $r$  can be seen in the second form of eqn (3).

In order to obtain a set of  $r$  and  $b$  values with correlation  $\rho$ , the parameters were chosen in the following way. The values of  $r$  and  $b$  were resubscripted as  $r_{wz}$  and  $b_{wz}$  so that the  $n$  values for each were contained in a two-dimensional array with  $w = 1, \dots, N$  and  $z = 1, \dots, N$ , where  $N^2 = n$ . Then for all  $z$ , the values of  $r_{wz}$  were set to the  $w/(n+1)$  percentile of a normal distribution with mean  $\bar{r}$  and variance  $\sigma_r^2 = (\bar{r}CV_r)^2$ . The  $b_{wz}$  were then chosen as the  $z/(n+1)$  percentile of a normal distribution that has been conditioned on the value of  $r_{wz}$ , with mean  $\bar{b} + (\sigma_b\rho/\sigma_r)(r_{wz} - \bar{r})$  and variance  $\sigma_b^2(1 - \rho^2)$ , where  $\sigma_b^2 = (\bar{b}CV_b)^2$ .

The final aspect of this single-patch model concerns extinctions and recolonizations. A genotype's abundance is set to zero if its abundance falls below 0.005. (Recall that the carrying capacity of a monomorphic host population is 1.0.) A group of host immigrants of a single genotype entered the population in each generation with probability  $\alpha$ . This simulates the effects of both migration and mutation, the processes that introduce genetic novelty into the local patch. The immigrants' genotype is equally likely to be any of the  $n$  possible races, so the average number of generations between immigrations by a particular race is  $n/\alpha$ . If the immigrant genotype is already present in the population, its abundance is increased by the truncation point, 0.005. If the immigrant genotype is absent, its abundance is set to 0.01. The same process occurs independently for the pathogens.

*Parameter values and design.* The following parameters were set for each run:  $c$ ,  $m$ ,  $s$ ,  $\bar{r}$ ,  $\bar{b}$ ,  $CV_r$ ,  $CV_b$ ,  $\rho$ ,  $\alpha$ , and  $n$ . A run begins with an empty patch, that is, no hosts or pathogens, and then the model is run for 2000 genera-

tions to initialize the system. For the following 4000 generations a variety of statistics are collected to answer the questions set out in the Introduction. All results presented below are from a full factorial design with three replicates. The parameter values are:  $c = 0.95, 1.00$ ;  $m = 0.05, 0.2$ ;  $s = 0.2, 0.8$ ;  $\bar{r} = 0.375, 0.625$ ;  $\bar{b} = 1.25, 1.75$ ;  $CV_r = 0.05, 0.2$ ;  $CV_b = 0.05, 0.2$ ;  $\rho = 0, \pm 0.25, \pm 0.5$ ;  $\alpha = 0.05, 0.1, 0.2$ ; and  $n = 4, 16, 64$ . This design has 5760 runs for each value of  $n$ .

Many of the analyses focus on the case  $n = 64$ . I believe that this case is the most realistic because it considers the dynamics when least constrained by the potential genetic variety. In those pathosystems controlled by major gene effects, populations sometimes harbour large amounts of genetic variation for virulence and resistance (Day, 1974; Burdon, 1987). This suggests that the potential genetic variety is rarely the factor that determines the level of variation observed. If, in a model, only four races are possible by mutation, then one cannot ask about the ecological and genetic interactions that maintain 10 or 20 varieties versus those that maintain only two.

*Summary statistics.* A variety of statistics was collected in each generation of a run. Each statistic was summarized over the 4000 generations of a run by its median value and its fifth and 95th percentiles. To summarize a statistic over a range of parameters, the mean median value and the mean fifth and 95th percentiles were used.

In the following sections the simulation results are presented for each of the six questions listed in the Introduction. The conclusions from these results are summarized in the Discussion.

### 1. Host abundance

The formula for the host equilibrium, eqn (2), predicts that the total abundance of hosts is  $s/b\gamma$ , which is approximately  $s/\bar{b}\gamma$  for biologically reasonable ranges for the cost of virulence. This fraction is the death-to-birth ratio for the pathogen population, therefore  $1 - s/\bar{b}\gamma$  is referred to as an index of pathogen pressure. This yields the prediction that total host abundance declines linearly with increasing pathogen pressure.

The prediction is simple and clear, so it may seem redundant to check it by computer simulation. The mathematical analysis requires, however, that the system is in stable equilibrium and that all  $2n$  races are present. These conditions are rarely met. In spite of these violations, the computer analysis shows that this particular prediction holds remarkably well.

There are four values of  $s/\bar{b}$  and three values of  $\gamma = (n-1)/n$  in the design. Median host abundance,  $H$ ,

is regressed against pathogen pressure, where the predicted regression coefficient is a negative one. The analysis was repeated for each  $n=4, 16, 64$ . In each case the regression coefficient was within 3 per cent of the predicted value. Each model explained at least 96 per cent of the total variance observed. Figure 1a shows the regression line for  $n=64$ .

Instability in the system may lead to epidemics and fluctuating host abundance. The theory presented

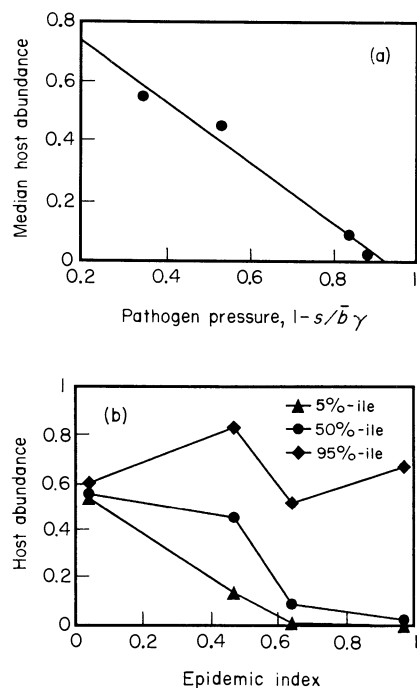


**Fig. 1** The median and range of host abundance over time as functions of the pathogen growth and death rates,  $b$  and  $s$ . (a) Host abundance decreases linearly with pathogen pressure (see text), with a slope near one. (b) Fluctuations in host abundance increase as the epidemic index,  $\delta\bar{b} - s$  increases. For all analyses in this paper  $\delta$  is set to  $2/3$  because that value yields an epidemic index near zero for the one case of stability observed. Each vertical slice shows the median and middle 90 per cent of the distribution of host abundances over time within a single patch.

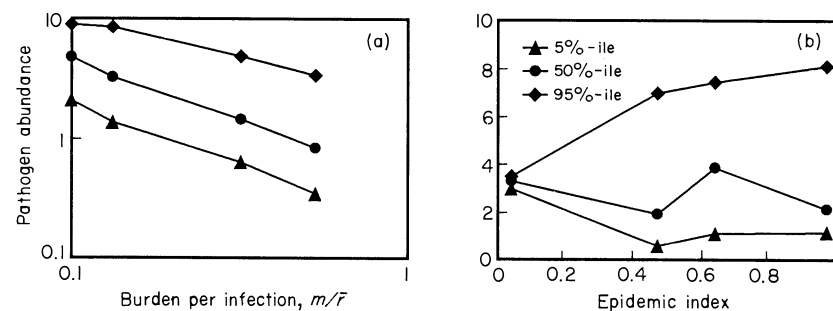


**Fig. 2** Factors influencing pathogen abundance and the frequency of disease. (a) Pathogen abundance declines with burden on host fitness caused per infection. Data are plotted on a log-log scale (see text). (b) Fluctuations over time as a function of the epidemic index.

above suggests that a symmetric system makes the transition from stable to unstable as the epidemic index  $\delta\bar{b} - s$  moves from negative to positive values, where at symmetric equilibrium  $\delta = (n-1)/n$ . The actual number of races in a real system will be much less than  $n$  when  $n$  is large, which suggests that a smaller value of  $\delta$  is needed in the index. The results were analysed from  $n=64$  and  $\delta = \frac{2}{3}$  chosen because it yielded an index near zero for the one case in which stability occurred ( $b=1.25$ ,  $s=0.8$ , and any other combination of parameters from the design). Figure 1b shows the means of the median and fifth and 95th percentiles of host abundance for the four  $(s, \bar{b})$  combinations from the design. Other simulation runs also support the conclusion that, for biologically realistic parameters, stability is controlled primarily by the difference between  $\delta\bar{b}$  and  $s$ .

In summary, these results support the usual Lotka–Volterra conclusion that total host abundance depends only on the ratio of death to birth rates of the pathogen population (Pielou, 1977, pp. 88–95). The results also show that the frequency of epidemics is controlled mostly by the difference between the pathogen birth and death rates.

## 2. Pathogen abundance and disease frequency

The total equilibrium abundance of pathogen races from eqn (3) is approximately

$$n\bar{p}^* \approx \frac{\bar{r}\{1 - [1 + (n-1)c]\bar{h}^*\}}{m\gamma}, \quad (5)$$

where  $\bar{h}^* = (\bar{s}/\bar{b})/(n-1)$ , and it is assumed that, for biologically reasonable parameters, the error in the approximation  $\bar{r}/\bar{b} \approx \bar{r}/\bar{b}$  is small.

The simulation results were analysed with respect to eqn (5) by fitting the regression model  $P = \text{intercept} + \bar{r}/m$ , where  $P$  is the median total abundance for a run. Other factors from eqn (5) explained little of the observed variance. This simple model explained more than 60 per cent of the observed variance for  $n=64$ ,

with similar results for the other values of  $n$ . The overall abundances declined slightly with increasing  $n$  at a rate determined approximately by the  $1/\gamma$  term in eqn (5).

An index for the hosts' fitness burden per infection is  $m/\bar{r}$ , the reduction in an infected individual's growth,  $m$ , divided by its intrinsic growth rate,  $\bar{r}$ . Figure 2a shows the relationship between the burden per infection and the median, fifth and 95th percentiles of the distribution of pathogen abundance. The data are plotted on a log-log scale to preserve the linear relationship between  $P$  and  $\bar{r}/m$  demonstrated in eqn (5). Figure 2b shows how pathogen abundance fluctuates as a function of the epidemic index,  $\delta b - s$ .

Disease frequency increases linearly with total pathogen abundance, apart from inoculations that result in resistant reactions. The results on pathogen abundance therefore provide a rough guide to the expected level of disease frequency.

### 3. Frequency of host resistance

The frequency of resistance is the number of inoculations to which the host is resistant,  $\sum_{i=1}^n h_i p_i$ , divided by the total number of inoculations,  $\sum_{i=1}^n h_i \sum_{k=1}^n p_k$ . In a symmetric model, this reduces to  $1/n$  at equilibrium. The average median frequency of resistance is 0.27 for  $n=4$  and 0.09 for  $n=16, 64$  when ignoring generations in which the frequency of resistance is zero. Frequencies of zero were ignored because they may be associated with the absence of hosts, the absence of pathogens, or the absence of resistant interactions.

Most of the observed variance can be explained by the main effects and first-order interactions for the parameters  $s$ ,  $b$ , and the migration-mutation parameter,  $\alpha$  (Fig. 3). Increasing migration-mutation,  $\alpha$ , causes a significant reduction in the frequency of resistance. Increased  $\alpha$  apparently makes it more difficult for hosts to escape pathogen attack. The reason for this is probably an asymmetry in the model that favours

pathogens: a pathogen can attack  $n-1$  host races, whereas a host is resistant to only one pathogen race.

### 4. Fitness burden caused by disease

The fitness burden per individual of the  $i$ th host race is  $\xi_i = (m/r_i)(\sum_{j=1}^n p_j - p_i)$ . The term  $(m/r_i)$  is the burden per infection, the morbidity and mortality relative to the potential growth rate. The pathogen abundance term is the number of infections suffered by an individual of the  $i$ th race. The average burden per individual is  $\bar{\xi} = \sum_{i=1}^n h_i \xi_i / \sum_{i=1}^n h_i$ , the fraction by which the host species's growth is reduced by pathogen load. In a symmetric model the above expressions for  $\bar{h}^*$  and  $\bar{p}^*$  can be used to obtain the prediction  $\bar{\xi} \approx 1 - [1 + (n-1)c]\bar{h}^*$ . Note from eqn (5) that  $\bar{\xi}/\gamma$  is simply the total abundance of pathogens multiplied by the burden per infection,  $m/\bar{r}$ .

If  $c$  is not too far from one, as would be expected for races of the same species, then at equilibrium for the full  $2n$ -dimensional system, the predicted average burden is  $\bar{\xi} \approx 1 - cs/\bar{b}\gamma$ . This is the reduction in host abundance relative to carrying capacity caused by the burden of disease. A burden of greater than one drives the host population to extinction.

The pathogen parameters,  $s$  and  $\bar{b}$ , and the migration-mutation rate,  $\alpha$ , explain at least 68 per cent of the variance in the median burden for the three values of  $n$ . (Frequencies of zero were ignored because they may be associated with the absence of hosts, the absence of pathogens, or the absence of resistant interactions.) For  $n=64$ , the main effects of the pathogen parameters  $s$  and  $\bar{b}$  explain more than 60 per cent of the variance in burden for the median, fifth and 95th percentiles.

No simple trend was observed between the burden measure and pathogen pressure,  $1 - s/\bar{b}\gamma$ , or the predicted burden value,  $1 - cs/\bar{b}\gamma$ . Instead, because the burden is sensitive to fluctuations in either host or pathogen abundance and race composition, the varia-

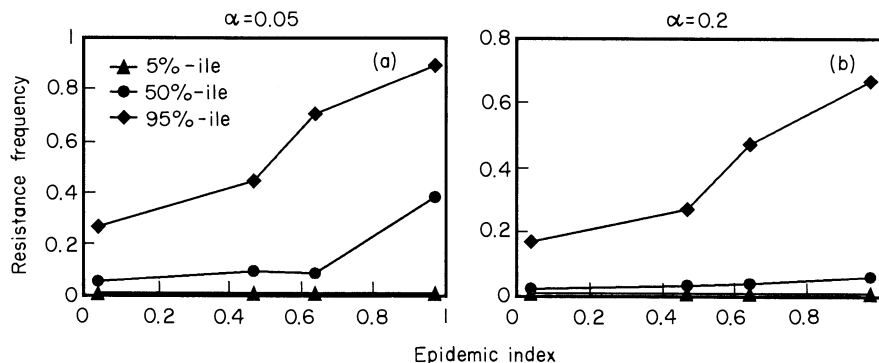
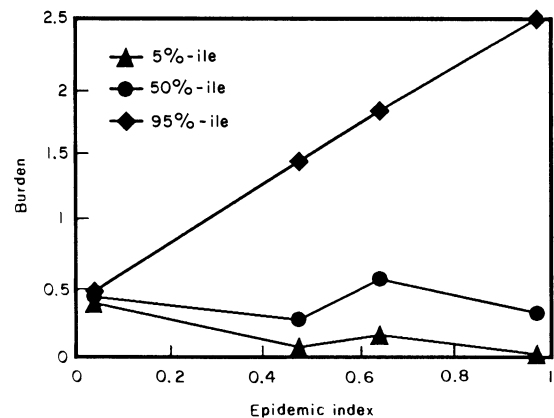


Fig. 3 The frequency of inoculations to which the host is resistant. The parameter  $\alpha$  is the migration-mutation rate.



**Fig. 4** The total fitness burden on the host population caused by disease as a function of the epidemic index.

tion in burden in each run increased with the epidemic index  $\delta\bar{b} - s$ . Burden values are plotted for  $n=64$  in Fig. 4, using  $\delta=2/3$ . The linear increase in burden for the 95th percentile occurred because the maximum burden increases linearly with the reproductive capacity of the pathogen population, which is the birth minus death rate, or  $\delta\bar{b} - s$ .

### 5. Host and pathogen polymorphism

The Shannon-Weaver index was used to measure diversity,  $D = -\sum_{i=1}^n \beta_i \log_2 \beta_i$ , where  $\beta_i$  is the frequency of the  $i$ th race (Shannon & Weaver, 1949). Maximum diversity occurs when all races equally

frequent, which yields  $D=2, 4, 6$  for  $n=4, 16, 64$ , or  $n=2^D$ .

The mean median values for hosts are 1.25, 1.43, 1.47 for  $n=4, 16, 64$ . Approximately 80 per cent of the variance in these values is explained by the main effects of  $s$ ,  $\bar{b}$ , and  $\alpha$ . Variation in the intrinsic rates of increase,  $CV_r$ , has little effect on host diversity because the hosts were typically kept well below carrying capacity by the pathogen load.

Figure 5a and b shows how host diversity fluctuates over time for  $n=64$ . The dashed line is the average diversity over time — the diversity index for the average frequency of the races over all 4000 generations of a run. The most striking result is that diversity at any point in time tends to decrease and become more variable as the potential for epidemics increases, whereas the average diversity increases with increasing intensity and variability in pathogen pressure. The reason is that, as epidemic pressure increases, a host race's success depends more on its ability to escape attack than on its intrinsic growth and competitive ability. Only a few races escape at any time and these dominate temporarily. However, these races are soon attacked and other resistant host races increase and dominate. Over time no particular host race has an advantage in escaping disease.

Variation in the parameters for pathogens did not cause much overall variance in diversity. Two sets of parameters affected diversity. First, instability and migration-mutation,  $s$ ,  $\bar{b}$ , and  $\alpha$ , caused only a small variance (Fig. 5c and d). Secondly, an increasing range

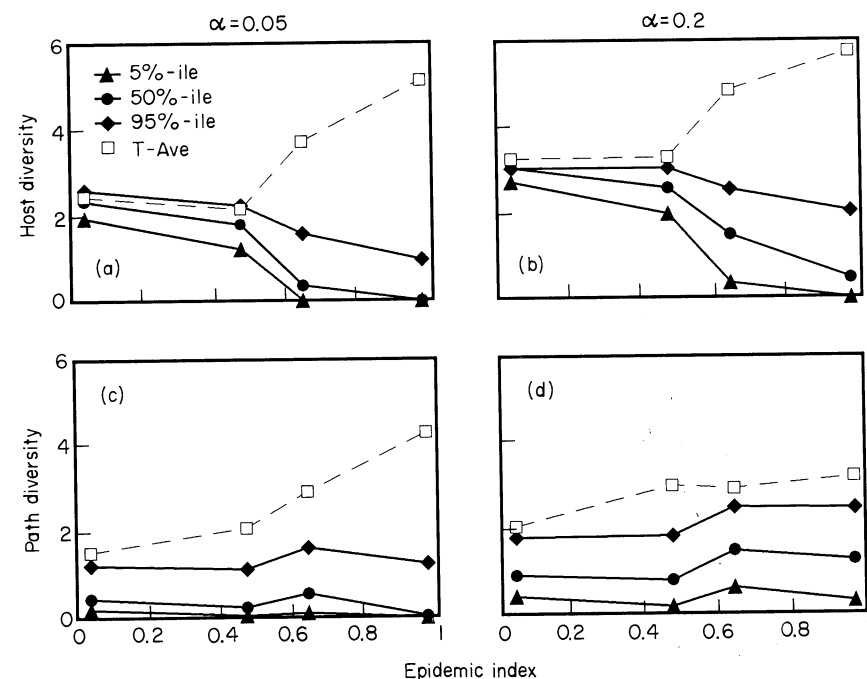


**Fig. 5** Shannon-Weaver diversity indices for hosts and pathogens. The dashed line is the diversity that occurs in the patch over time.

in the cost of virulence values,  $b$ , reduced pathogen diversity by increasing the opportunity for selection and thus for dominance by the superior races. For example, an increase in  $n$  or  $CV_b$  raised the range in  $b$  and reduced diversity.

The diversity index  $D$  depends on both the number of races and their relative frequencies. The mean median values for the number of host races present, following the filled-circle parameter combinations in Fig. 5b from low to high epidemic index values, are 11.3, 7.6, 3.7, and 1.6. The values for pathogens following the parameters for filled circles in Fig. 5d are 5.8, 3.9, 10.3, and 7.5.

The numbers of races compared with the diversity values in the figures suggest that the pathogens tend to have a more skewed distribution of race frequencies than the hosts. This is consistent with the above conclusion that variation in  $b$  plays a more important role for pathogen success than does variation in  $r$  for the hosts. In this model, the indirect competition between pathogens via their effects on host abundance appears to be more potent than the direct competition between hosts for limiting resources.

## 6. Distributions of the costs of resistance and virulence

The influx of genetic variation by migration and mutation was determined by the means,  $\bar{r}$  and  $\bar{b}$ , the standard deviations,  $CV_r$  and  $CV_b$ , and the correlation  $\rho$  between the costs of resistance and virulence. Selec-

tion within species tends to increase the observed averages of  $r$  and  $b$  above the mutational average, reducing the costs of resistance and virulence. This tendency may be opposed by coevolution, with hosts selected that have a high level of resistance to the dominant pathogen and pathogens selected that have a broad virulence range over the available hosts.

In each generation, the deviation of the observed average of  $r$  and  $b$  from the mutational mean was measured. For example,  $DEV_r = (AVE_r - \bar{r}) / (\bar{r} CV_r)$  is the number of standard deviations of the observed average of  $r$  from the mutational average, where the standard deviation is the square root of the mutational variance. A similar measure was constructed for  $b$ . For  $n = 64$ , the epidemic index and the migration-mutation rate explained most of the variation in these measures (Fig. 6). The host and pathogen populations maintained little variation in the costs of resistance and virulence when the system was stable (low epidemic index), and the observed averages for  $r$  and  $b$  were near the maximum that occurred by mutation.

If the epidemic index was high, selection within species had little effect on the mean and variation in the costs of resistance and virulence (Figs 5 and 6). Only when migration-mutation was high could the pathogens replace the frequent extinctions of dominant races with recolonizing races that also have a low cost of virulence (Fig. 6d).

In summary, when instability and epidemics occur there is little association between the cost of resistance or virulence and the success of a race. The temporary

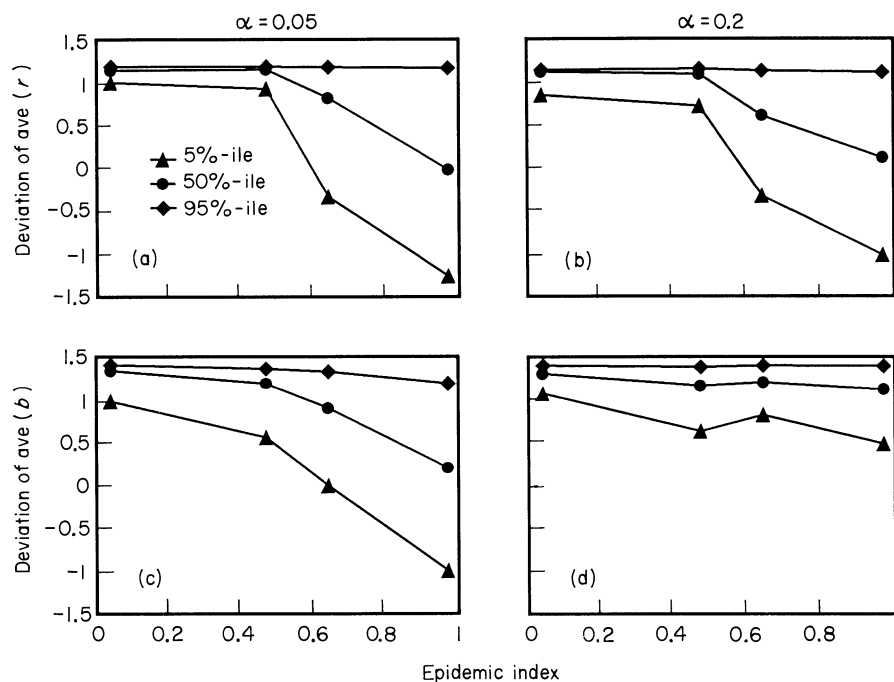


**Fig. 6** The change in the average costs of resistance and virulence. Selection within populations increases the deviation, whereas coevolutionary interactions tend to diversify the values over time.

success of a race depends mainly on its ability to avoid resistant hosts or virulent pathogens and on luck in arriving in a patch that is favourable for colonization and rapid growth.

## Discussion

### *Answers to the six introductory questions*

1. *What determines host abundance?* Host abundance declines linearly with an index of pathogen pressure,  $1 - s/b\gamma$ , where  $s$  is the death rate of the pathogens and  $b\gamma$  is the average birth and recruitment rate of the pathogen population (Fig. 1a). Host abundance does not depend on the hosts' growth, intraspecific competition, or the morbidity and mortality associated with disease, because the pathogens tend to increase until the pressure of disease balances the hosts' growth. For example, faster host growth leads to more pathogens and disease, not more hosts (Fig. 2a). Host abundance may fluctuate considerably over time (Fig. 1b). The range of fluctuation is determined by the rate of increase of the pathogen,  $\delta\bar{b} - s$ , where  $\delta$  is an undetermined constant that depends mainly on the average host range of the pathogens. The pathogen rate of increase is referred to as the epidemic index.

2. *What determines pathogen abundance?* Pathogen abundance is inversely proportional to the fitness burden per infection,  $m/\bar{r}$ , where  $m$  is the morbidity and mortality per infection and  $\bar{r}$  is the intrinsic rate of increase of the host population (Fig. 2a). For example, a mild disease (small  $m$ ) supports many more pathogens because the pathogens increase until the disease balances the host's growth. The amount of fluctuation in pathogen abundance is determined by the epidemic index (Fig. 2b).

3. *What determines the frequency of resistance?* The frequency of resistance varies considerably over time (Fig. 3). These fluctuations increase with an increasing frequency of epidemics because the changing fortunes of the host population that characterize epidemics depend on the rise and fall in the frequency of resistant races. Resistance frequency declines with an increasing influx of genetic novelty by immigration and mutation because, in this model, the host range of pathogens is broad and the resistance specificity of the hosts is narrow. The results in Fig. 3 also suggest caution when testing the hypothesis of pathogen specialization, in which the most abundant pathogen races in each spatially distinct patch are predicted to be those virulent on the locally dominant host races (Parker, 1985). Figure 3 shows that the same patch at different times

may strongly support or reject the hypothesis of pathogen specialization.

4. *What determines the burden of disease on host fitness?* The observed burden is defined as the proportional decrease in potential host growth caused by disease. In a stable system without epidemics, host abundance is approximately the carrying capacity multiplied by one minus the burden (compare the values at low epidemic index in Fig. 1b and Fig. 4). When epidemics occur, fluctuations in burden follow changes in disease frequency which in turn depend mainly on pathogen abundance (compare Fig. 2b and Fig. 4).

5. *What determines genetic diversity in hosts and pathogens?* The genetic variability of hosts at a particular point in time and space declines as epidemics become more frequent and intense (Fig. 5a and b). By contrast, the variability in one location over time increases greatly with increasing epidemics (dashed line in Fig. 5a and b). Pathogen diversity at a particular point in time and space is not sensitive to the epidemic index (Fig. 5c and d). The hosts tend to have a fairly even distribution of race frequencies, whereas the pathogens tend to have a skewed distribution. (See data presented above on the number of races present compared with the diversity index.)

6. *What determines the cost of resistance and virulence?* The distributions of the cost of resistance and virulence provide further information on genetic variability. The dominant host and pathogen races have the lowest costs when the epidemic index is low (Fig. 6). With increasing epidemic pressure, the main selective force on a host is escaping from disease, and the distribution of cost values approaches the mutational distribution (Fig. 6a and b). If the epidemic index is high, an observed polymorphism and cost is more likely to represent transience (Leonard & Czocho, 1980) than balancing selection ('stabilizing selection' in Vanderplank, 1963, 1968). For pathogens, there is an interesting interaction between the epidemic index and the migration-mutation rate,  $\alpha$ . When  $\alpha$  is sufficiently high, the dominant pathogen races have a reduced cost of virulence over all ranges of the epidemic index (Fig. 6c and d, and the dashed lines in Fig. 5c and d). The analogous reduction in costs does not occur in hosts (Fig. 6a and b). It appears that competition among pathogen races is more intense than competition among host races.

### *Assumptions of the model*

*Time.* The dynamics of species interactions can depend strongly on the time intervals between successive periods of birth, death, and infection (e.g. May, 1975; Fleming, 1980). One mathematical technique is to consider events that occur continuously. In continuous interactions, an increase in the pathogen population causes an instantaneous increase in the number of infections and a decrease in the growth rate of the host population. This reduction in host growth immediately lowers the rate at which new infections are formed and therefore slows the growth of the pathogen population. Because hosts and pathogens constantly adjust to each other, there is little chance of sizeable spurts or crashes in population sizes, and thus little chance of epidemics.

This model was chosen as one in which events such as birth, death and infection are assumed to occur in discrete time intervals. Inoculation and infection occur once during each time period (season). Hosts compete with each other, suffer disease, reproduce, and die, and in consequence contribute a certain number of individuals to the next season. Pathogens infect, reproduce, and die, or else fail to attach themselves and remain in a resting state, and in consequence contribute a certain number of new progeny and surviving spores. Because the host–pathogen interaction is determined by population numbers at the beginning of the season, the pathogens may build up a very large population size while the host numbers remain steady or decline slightly. In the next season, disease will be rampant, host reproduction will suffer, and a population crash will follow. In the next season, the pathogens will have a few hosts to attack, and their population will decay at a rate determined mainly by spore survival.

Neither the discrete model nor the continuous model are realistic. Either can be made more realistic by adding explicit assumptions about the time delays between interactions.

*Space.* The Lotka–Volterra model assumes random mixing of host and pathogen genotypes in each season. The rate of interaction between particular host and pathogen races is the product of their abundances. This ignores the spatial dimension of disease that occurs on two scales. In a local area, the spread of disease depends on the mechanisms of pathogen dispersal and on the mechanisms and timing of acquired immunity.

Globally, the host–pathogen interaction typically occurs in many separate patches, with varying degrees of migration between these patches. The strength of coupling (migration) among patches has a very strong effect on global dynamics (Levins & Culver, 1971; Slatkin, 1974; Frank, 1989; Burdon *et al.*, 1989, 1990).

For example, if genotypes turn over within each patch because of host–pathogen coevolution, then the genetic diversity across all patches may be very high even though it is low in each patch. A hint of this can be seen in Fig. 5, where the dashed line shows that the diversity over time in each patch is high even though diversity is low at any point in time. If the patches are at different stages of turnover, then the spatial diversity at one time may be similar to the temporal diversity in each patch (Frank, 1989; A. M. Jarosz & J. J. Burdon, unpublished comments).

The local and global interactions are important exceptions to the Lotka–Volterra assumptions. For local interactions, however, the Lotka–Volterra model provides the basis for understanding more complex epidemiology; the mathematical reasons for this are summarized by May (1975, p. 42). Globally, multi-patch models may often behave as a set of one-patch interactions loosely coupled by migration (S. A. Frank, unpublished results), so the dynamics of single patches must be studied thoroughly before proceeding to more complex models.

*Genetics.* The model assumes asexual haploid genetics with each host allele conferring resistance to only one of  $n$  pathogen alleles. This is the barest representation of gene-for-gene genetics. More realistic genetic assumptions will complicate the simple results presented here. However, the measures of pathogen pressure, burden per infection, and the epidemic index depend mainly on ecological parameters such as birth and death rates. Even in complex genetic models these measures will probably maintain their power to explain the amount of genetic diversity.

### *Relation to past work*

Many published genetic models on host–pathogen coevolution assume fixed population sizes. These are not reviewed here because a joint analysis of abundance (ecology) and genetics is required to understand the maintenance of polymorphism (May & Anderson, 1983; for reviews of genetic models, see Levin, 1983; Seger, 1988; Hamilton, 1991). Ecological models that examine abundance and diversity of interacting species provide a starting point for analysing genetic diversity because interacting species are formally analogous to single-locus haploid genetics.

There is a vast ecological literature on Lotka–Volterra dynamics. The equilibrium abundance results for a one-host and one-pathogen system can be found in most texts on ecology (e.g. Pielou, 1977; historical background can be found in Scudo & Ziegler, 1978). The results correspond to eqn (2) and eqn (5), with

$n = \gamma = 1$ . The majority of theoretical literature on multi-dimensional interactions concerns whether a system is stable or unstable. This theory would be particularly valuable if there were key parameters that move systems across the stability–instability boundary, and these parameters can be estimated.

Little theoretical work has been devoted to the distributional properties of abundance and polymorphism. Predictions and observations on statistical distributions are required to test hypotheses about fluctuating quantities. For example, Fig. 2a shows that the burden part of the equation for equilibrium pathogen abundance, eqn (5), can explain the main trends in observed pathogen abundance. Over time, however, the observed pathogen abundance fluctuates over nearly an order of magnitude. Methods to analyse time-series data have recently been developed and applied to epidemics. See Olsen & Schaffer (1990) and Sugihara & May (1990).

### Generating comparative hypotheses

The six questions and the measures for coevolutionary interaction form a basis for comparative hypotheses about the causes of genetic diversity. For example, Fig. 5 suggests that as the epidemic index rises, the median amount of host polymorphism declines but the temporal fluctuations in polymorphism increase. The epidemic index is the potential rate of increase of the pathogen. Very different rates of increase are known from different plant pathogens, ranging from 0.1 to 0.5 per day for pathogens that have several reproductive cycles per season such as wheat stem rust and tobacco mosaic virus to 0.8–1.2 per year for Dutch elm disease and chestnut blight (Agrios, 1988, pp. 60, 61, 168).

Developing a consistent time metric is a problem for testing the association between these rates of pathogen increase and the relative levels of genetic diversity. For example, although Dutch elm disease increases at a rate of only 0.8 per year, the elm had a long generation time. The reproductive rate of this disease relative to its host's reproductive period may approach that of wheat stem rust, a relatively short-generation pathogen on a short-generation host. In spite of the large differences in absolute growth, these two systems may have similar epidemic indices. The time metric of the parameters must be borne in mind when relating the theory to data. With this caveat, the model presented here introduces a comparative theory for genetic diversity in host–pathogen coevolution.

### Acknowledgment

Mark Andersen provided helpful comments on an earlier version of the manuscript. My research was

supported by NIH grants GM42403 and BRSO-S07-RR07008 and NSF grant BSR-9057331.

### References

- AGRIOS, G. N. 1988. *Plant Pathology*. Academic Press, New York.
- BURDON, J. J. 1987. *Diseases and Plant Population Biology*. Cambridge University Press, Cambridge.
- BURDON, J. J., JAROSZ, A. M. AND KIRBY, G. C. 1989. Pattern and patchiness in plant–pathogen interactions — causes and consequences. *Ann. Rev. Ecol. Syst.*, **20**, 119–136.
- BURDON, J. J., BROWN, A. H. D. AND JAROSZ, A. M. 1990. The spatial scale of genetic interactions in host–pathogen coevolved systems. In: Burdon, J. J. and Leather, S. R. (eds), *Pests, Pathogens and Plant Communities*, Blackwell Scientific Publications, Oxford, pp. 233–247.
- DAY, P. R. 1974. *Genetics of Host–Parasite Interaction*. W. H. Freeman, San Francisco.
- FLEMING, R. A. 1980. Selection pressures and plant pathogens: robustness of the model. *Phytopathology*, **70**, 175–178.
- FLOR, H. H. 1956. The complementary genic systems in flax and flax rust. *Adv. Genet.*, **8**, 29–54.
- FRANK, S. A. 1989. The evolutionary dynamics of cytoplasmic male sterility. *Am. Nat.*, **133**, 345–376.
- HAMILTON, W. D. 1991. Memes of Haldane and Jayakar in a theory of sex. *J. Genet.* (in press).
- LEONARD, K. J. AND CZOCHOR, R. J. 1980. Theory of genetic interactions among populations of plants and their pathogens. *Ann. Rev. Phytopathol.*, **18**, 237–258.
- LEVIN, S. A. 1983. Some approaches to the modelling of coevolutionary interactions. In: Nitecki, M. H. (ed.), *Coevolution*, University of Chicago Press, Chicago, pp. 21–65.
- LEVINS, R. AND CULVER, D. 1971. Regional coexistence of species and competition between rare species. *Proc. Natl. Acad. Sci., USA*, **68**, 246–248.
- MAY, R. M. 1975. *Stability and Complexity in Model Ecosystems*, 2nd edn. Princeton University Press.
- MAY, R. M. AND ANDERSON, R. M. 1983. Epidemiology and genetics in the coevolution of parasites and hosts. *Proc. R. Soc. Lond. B*, **219**, 281–313.
- OLSEN, L. F. AND SCHAFFER, W. M. 1990. Chaos versus noisy periodicity: alternative hypotheses for childhood epidemics. *Science*, **249**, 499–504.
- PARKER, M. A. 1985. Local population differentiation for compatibility in an annual legume and its host-specific fungal pathogen. *Evolution*, **39**, 713–723.
- PIELOU, E. C. 1977. *Mathematical Ecology*, 2nd edn. Wiley, New York.
- SCUDO, F. M. AND ZIEGLER, J. R. 1978. *The Golden Age of Theoretical Ecology*. Springer-Verlag, New York.
- SEGER, J. 1988. Dynamics of some simple host–parasite models with more than two genotypes in each species. *Phil. Trans. R. Soc. Lond. B*, **319**, 541–555.
- SHANNON, C. E. AND WEAVER, W. 1949. *The Mathematical Theory of Communication*. University of Illinois Press, Urbana.
- SLATKIN, M. 1974. Competition and regional coexistence. *Ecology*, **55**, 128–134.

- SUGIHARA, G. AND MAY, R. M. 1990. Nonlinear forecasting as a way of distinguishing chaos from measurement error in time series. *Nature*, **344**, 734–741.
- VANDERPLANK, J. E. 1963. *Plant Diseases: Epidemics and Control*. Academic Press, New York.
- VANDERPLANK, J. E. 1968. *Disease Resistance in Plants*. Academic Press, New York.
- WOLFRAM, S. 1988. *Mathematica: A System for Doing Mathematics by Computer*. Addison–Wesley, Redwood, California.